

# Quintessential kination and leptogenesis

Eung Jin Chun<sup>1,2</sup> and Stefano Scopel<sup>1</sup>

<sup>1</sup> Korea Institute for Advanced Study, 207-43 Cheongryangri-dong  
Dongdaemun-gu, Seoul 130-722, Korea

<sup>2</sup> Michigan Center for Theoretical Physics, Department of Physics,  
University of Michigan, Ann Arbor, MI 48109, USA  
E-mail: [ejchun@kias.re.kr](mailto:ejchun@kias.re.kr) and [scopel@kias.re.kr](mailto:scopel@kias.re.kr)

Received 16 July 2007

Accepted 24 September 2007

Published 15 October 2007

Online at [stacks.iop.org/JCAP/2007/i=10/a=011](http://stacks.iop.org/JCAP/2007/i=10/a=011)

doi:10.1088/1475-7516/2007/10/011

**Abstract.** Thermal leptogenesis induced by the  $CP$ -violating decay of a right-handed neutrino (RHN) is discussed against the background of quintessential kination, i.e., in a cosmological model where the energy density of the early Universe is assumed to be dominated by the kinetic term of a quintessence field during some epoch of its evolution. This assumption may lead to very different observational consequences compared to the case of a standard cosmology where the energy density of the Universe is dominated by radiation. We show that, depending on the choice of the temperature  $T_r$  above which kination dominates over radiation, all situations between the strong and the superweak wash-out regimes are equally viable for leptogenesis, even with the RHN Yukawa coupling fixed to provide the observed atmospheric neutrino mass scale  $\sim 0.05$  eV. For  $M \lesssim T_r \lesssim M/100$ , i.e., when kination stops to dominate at a time which is not much later than when leptogenesis takes place, the efficiency of the process, defined as the ratio between the produced lepton asymmetry and the amount of  $CP$  asymmetry in the RHN decay, can be larger than in the standard scenario of radiation domination. This possibility is limited to the case when the neutrino mass scale is larger than about 0.01 eV. The superweak wash-out regime is obtained for  $T_r \ll M/100$ , and includes the case when  $T_r$  is close to the nucleosynthesis temperature,  $\sim 1$  MeV. In this latter case the efficiency for leptogenesis is strongly suppressed, but can still explain the baryon asymmetry observed in the Universe when a resonant  $CP$  asymmetry of order 1 is assumed. Irrespective of  $T_r$ , we always find a sufficient window above the electroweak temperature  $T \sim 100$  GeV for the sphaleron transition to thermalize, so that the lepton asymmetry can always be converted to the observed baryon asymmetry.

**Keywords:** dark energy theory, baryon asymmetry

**ArXiv ePrint:** [0707.1544](https://arxiv.org/abs/0707.1544)

---

**Contents**

<b>1. Introduction</b>	<b>2</b>
<b>2. Kination and leptogenesis</b>	<b>3</b>
<b>3. Supersymmetric kination leptogenesis</b>	<b>5</b>
<b>4. Properties of leptogenesis: kination versus radiation</b>	<b>8</b>
4.1. Superweak wash-out regime . . . . .	8
4.2. Strong wash-out regime . . . . .	10
4.3. The efficiency in terms of $K$ or $(z_r, \tilde{m})$ . . . . .	13
<b>5. Conclusions</b>	<b>15</b>
<b>Acknowledgment</b>	<b>16</b>
<b>References</b>	<b>16</b>

---

**1. Introduction**

Present observations strongly favor the existence of dark energy, which contributes a fraction  $\Omega_{\text{DE}} \simeq 0.7$  to the closure density. This dark energy component in the present Universe can be explained by modifying the standard cosmology with the introduction of a slowly evolving scalar field called quintessence [1]. This approach has been shown to have ‘tracking solutions’ [2] that solve the so-called coincidence problem suffered by a pure cosmological constant, namely explaining in a natural way why radiation and dark energy provide comparable contributions to the energy budget of the present Universe, in spite of having very different time evolutions. An open possibility in this scenario is the existence of an early era of kination domination, during which the Universe is dominated by the kinetic energy of the quintessence field. During this era, the expansion rate of the Universe is larger compared to the usual radiation domination case. An interesting consequence of this fact is that the relic abundance of a cold dark matter candidate can be significantly enhanced compared to the canonical prediction [3], because its decoupling time from the plasma is anticipated. In this way, for models with high detection rates, the relic density that is usually small in the standard case can be brought back to the range compatible with observation. This leads to interesting phenomenological implications for the LHC and other future collider or astrophysics experiments. Another interesting prediction of the kination domination scenario in inflationary models is the absence of a measurable tensor perturbation induced  $B$ -mode CMB polarization, which can be tested in the next-generation CMB experiments [4].

In this paper, we investigate the impact of the quintessential kination scenario on the properties of the thermal leptogenesis induced by the  $CP$ -violating decay of a right-handed neutrino (RHN),  $N$  [5]. In particular, when the RHN Yukawa coupling is fixed in order to explain the observed atmospheric neutrino mass scale  $\simeq 0.05$  eV through the seesaw mechanism, leptogenesis is known to proceed in the strong wash-out regime for a standard cosmology. As will be shown in the following, similarly to the case for the

relic density of a thermal relic, the faster expansion rate in the early Universe due to kination dominance can modify the predictions for the standard leptogenesis scenario, even by several orders of magnitude. As a consequence of this, all situations between the strong and the superweak wash-out regime are equally viable for leptogenesis in the presence of kination domination. In particular, as explained in the following sections, in all cases successful leptogenesis can in principle be achieved. However, except for a relatively limited choice of the parameters, this will imply the need to invoke a resonant  $CP$  asymmetry of order 1.

The paper is organized as follows. In section 2 the main features of the quintessential cosmological scenario are summarized, and the basic requirements for kination domination at early times are discussed. In section 3 thermal leptogenesis is discussed in the context of an MSSM model supplemented by heavy right-handed neutrino supermultiplets with  $CP$ -violating decays, and the relevant Boltzmann equations are introduced. Section 4 is devoted to our discussion, where the solutions for the Boltzmann equations of leptogenesis for a kination dominated Universe are compared to those for the standard radiation dominated case. We summarize our conclusions in section 5.

## 2. Kination and leptogenesis

Let us begin with a brief summary of the cosmological behavior of kination. The kination regime is attained when, in the energy–momentum tensor of the quintessence field  $\phi$  (assumed here as spatially constant):  $T_{\mu\nu} = \partial_\mu\phi(\partial\mathcal{L}/\partial\partial^\nu\phi) - g_{\mu\nu}\mathcal{L}$ , the kinetic term  $\dot{\phi}^2/2$  dominates over the potential term  $V(\phi)$ , so that

$$w \equiv \frac{p}{\rho} = \frac{(\dot{\phi}^2/2) - V(\phi)}{(\dot{\phi}^2/2) + V(\phi)} \rightarrow 1. \quad (1)$$

Equation (1) must be compared to the corresponding values for radiation ( $w = 1/3$ ), vacuum ( $w = -1$ ) and pressureless dust ( $w = 0$ ). The energy density of the Universe scales like  $\rho \propto a^{-3(1+w)}$ , which, in particular, implies

$$\begin{aligned} \rho_{\text{rad}} &\propto a^{-4} && \text{(radiation),} \\ \rho_{\text{kin}} &\propto a^{-6} && \text{(kination).} \end{aligned} \quad (2)$$

In the following, we will assume that, in the epoch after reheating which is relevant to thermal leptogenesis, the energy density of the Universe is dominated by the sum of the above two components,  $\rho = \rho_{\text{rad}} + \rho_{\text{kin}}$ , with the boundary condition

$$\rho_{\text{kin}}(T_r) = \rho_{\text{rad}}(T_r), \quad (3)$$

where the kination–radiation equality temperature  $T_r$  is in principle a free parameter, with the only constraint  $T_r \gtrsim 1$  MeV, in order not to spoil big-bang nucleosynthesis. Equations (2) and (3) imply

$$\rho(T) = \rho_{\text{rad}}(T) + \rho_{\text{rad}}(T_r) \left(\frac{a_r}{a}\right)^6, \quad (4)$$

where  $\rho_{\text{rad}}(T) = \pi^2/30g_*T^4$ , and  $g_*$  is the number of relativistic degrees of freedom. Assuming an isentropic expansion of the Universe,  $(a^3s) = \text{constant}$ , with  $s =$

$2\pi^2/45g_*T^3$ , we get

$$g_*a^3T^3 = g_{*r}a_r^3T_r^3 \rightarrow \left(\frac{a_r}{a}\right)^6 = \left(\frac{g_*}{g_{*r}}\right)^2 \left(\frac{T}{T_r}\right)^6, \quad (5)$$

where  $a_r$  and  $g_{*r}$  are the values of  $a$  and  $g_*$  at temperature  $T_r$ . Thus one finds the dependence of  $\rho$  on the temperature  $T$  as

$$\rho(T) = \frac{\pi^2}{30}g_*T^4 \left(1 + \frac{g_*}{g_{*r}} \left(\frac{T}{T_r}\right)^2\right). \quad (6)$$

The above form of the energy density drives the expansion of the Universe through the Hubble parameter given by

$$H(T) = 1.66\sqrt{g_*}\frac{T^2}{m_{\text{pl}}}\sqrt{1 + \frac{g_*}{g_{*r}} \left(\frac{T}{T_r}\right)^2}, \quad (7)$$

where  $m_{\text{pl}} = 1.22 \times 10^{19}$  GeV. By introducing the non-dimensional quantity  $z \equiv M/T$ , where  $M$  is the mass of the heavy neutrino producing leptogenesis, the scaling of  $H$ , which will be relevant to the solution of the Boltzmann equation discussed in the next section, can be expressed in the simple form

$$H(z) = \sqrt{\frac{z^2 + z_r^2}{1 + z_r^2}} \frac{H_1}{z^3}, \quad (8)$$

where  $H_1 \equiv H(z = 1)$  and  $z_r \equiv \sqrt{(g_*/g_{*r})}M/T_r$ .

The main consequence of equations (7) and (8) is that, whenever  $T > T_r$ , the expansion rate is dominated by kination, and can be much faster compared to the radiation case. In particular, taking  $T_r = 1$  MeV as an order of magnitude value for the nucleosynthesis temperature,  $g_{*r} = 10.75$  and  $g_*(T) = 228.75$  in the supersymmetric standard model, we get

$$H(T) \simeq 0.95 \times 10^4 \text{ GeV} \left(\frac{3.28 \text{ MeV}}{\sqrt{g_{*r}}T_r}\right) \left(\frac{T}{10^6 \text{ GeV}}\right)^3. \quad (9)$$

This value must be compared to the rate of gauge interactions, that ensure thermalization after reheating. Their scattering rate is approximately given by  $\Gamma_{\text{gauge}} \approx \alpha^2 T$ , so that the requirement  $\Gamma_{\text{gauge}} > H$  leads to the following upper limit on the reheat temperature and thus on the RHN mass:

$$M \simeq T < 3.4 \times 10^5 \left(\frac{\sqrt{g_{*r}}T_r}{3.28 \text{ MeV}}\right)^{1/2} \text{ GeV}, \quad (10)$$

for  $\alpha = 1/30$ . The bound of equation (10) implies that in the quintessential kination scenario thermal leptogenesis requires a RHN mass which is typically lower than in the standard case  $M \gtrsim 10^9$  GeV [6]. Of course, the above constraint on  $M$  can be relaxed when  $T_r \gg 1$  MeV, as the conventional picture of radiation domination is recovered for  $z_r \rightarrow 0$ . Moreover, in order to allow the conversion of the lepton asymmetry to the baryon asymmetry, the electroweak sphaleron interaction must be in thermal equilibrium before the electroweak phase transition. Taking the order of magnitude estimate of the sphaleron

interaction rate  $\Gamma_{\text{sp}} \sim \alpha^4 T$  [7], the condition  $\Gamma_{\text{sp}} > H$  reduces the above constraint (10) by an additional factor  $\alpha$ :

$$T < 10^4 \left( \frac{\sqrt{g_{*r}} T_r}{3.28 \text{ MeV}} \right)^{1/2} \text{ GeV}. \quad (11)$$

Therefore, we get a sufficient window for the sphaleron transition to thermalize above the electroweak temperature  $T \sim 100 \text{ GeV}$  even for  $T_r \simeq 1 \text{ MeV}$ .

### 3. Supersymmetric kination leptogenesis

In this paper we wish to discuss thermal leptogenesis in the minimal supersymmetric extension of the standard model (MSSM) supplemented by right-handed neutrino supermultiplets, i.e. the model described by the following superpotential:

$$\mathcal{W} = \mathcal{W}_{\text{MSSM}} + \frac{1}{2} N^c M N^c + y H_2 L N^c. \quad (12)$$

This scenario has been extensively studied in the literature [8, 9] in a conventional cosmological set-up where the energy density of the early Universe is dominated by radiation. We wish now to discuss leptogenesis in the scenario of kination domination introduced in the previous section. Let us remark that our results are also applicable to the non-supersymmetric case without any qualitative change.

In the MSSM, the decay rate of a RHN is given by  $\Gamma_d = |y|^2 M / 4\pi$  where  $y$  is the neutrino Yukawa coupling. Introducing as usual the effective neutrino mass scale given by

$$\tilde{m} \equiv |y|^2 \frac{\langle H_2 \rangle^2}{M}, \quad (13)$$

and using equation (8), we can get the ratio  $K \equiv \Gamma_d / H(z = 1)$ :

$$K = \frac{63.78}{\sqrt{1 + z_r^2}} \left( \frac{\tilde{m}}{0.05 \text{ eV}} \right). \quad (14)$$

We recall that the standard cosmology is recovered in the above equation when  $z_r \ll 1$ , and thus leptogenesis proceeds in the strong wash-out regime,  $K \gg 1$ , for  $\tilde{m}$  equal to the observed atmospheric neutrino mass scale. The situation changes for kination domination, where  $z_r \gg 1$ . In particular, putting numbers in the above equation one gets

$$K = 1.38 \times 10^{-6} \left( \frac{10^4 \text{ GeV}}{M} \right) \left( \frac{\tilde{m}}{0.05 \text{ eV}} \right) \left( \frac{\sqrt{g_{*r}} T_r}{3.28 \text{ MeV}} \right). \quad (15)$$

Thus, if kination dominates the energy density of the Universe until nucleosynthesis, leptogenesis is in the superweak wash-out regime,  $K \lll 1$ , even when  $\tilde{m} \simeq 0.05 \text{ eV}$ . On the other hand, assuming  $T_r \gg 1 \text{ MeV}$ , higher values of  $K$  can be attained, so that a broad range of different scenarios are possible. However, as will be shown in the discussion of section 4, an upper bound  $K \lesssim 10$  exists if kination has to play any role for leptogenesis.

The Boltzmann equations that drive leptogenesis involve the comoving densities  $Y_i(z = M/T) \equiv n_i / s(z)$ , with  $n_i$  the density of the species  $i$ ,  $s$  the entropy density, and  $i = N$  (heavy Majorana neutrinos),  $\tilde{N}$  (sneutrinos),  $\tilde{N}^\dagger$  (anti-sneutrinos),  $l$  (leptons),  $\bar{l}$  (anti-leptons),  $\tilde{l}$  (sleptons) and  $\tilde{l}^\dagger$  (anti-sleptons). We do not study the additional degrees

of freedom  $h_2, h_2^\dagger$  (Higgs bosons) and  $\tilde{h}$  (higgsinos) since their densities are constrained to be very close to  $\tilde{l}, \tilde{l}^\dagger$  and  $l$ . Moreover, all other light degrees of freedom are assumed in thermal equilibrium. We recall that, as discussed in [10], taking the chemical potentials of all particles in the plasma into account in the Boltzmann equations would enhance the washout process by a factor  $\mathcal{O}(1)$ . It is convenient to introduce the following adimensional densities:

$$\begin{aligned} N(z) &\equiv \frac{Y_N(z)}{Y_N^{\text{eq}}(z=0)}, & \tilde{N}(z) &\equiv \frac{Y_{\tilde{N}}(z)}{Y_{\tilde{N}}^{\text{eq}}(z=0)}, & \tilde{N}^\dagger(z) &\equiv \frac{Y_{\tilde{N}^\dagger}(z)}{Y_{\tilde{N}^\dagger}^{\text{eq}}(z=0)}, \\ \tilde{N}_\pm &\equiv \tilde{N}(z) \pm \tilde{N}^\dagger(z), & L(z) &\equiv \frac{Y_l(z) - Y_{\tilde{l}}(z)}{Y_l^{\text{eq}}(z=0)}, & \tilde{L}(z) &\equiv \frac{Y_{\tilde{l}}(z) - Y_{\tilde{l}^\dagger}(z)}{Y_{\tilde{l}}^{\text{eq}}(z=0)}. \end{aligned} \quad (16)$$

The Boltzmann equations of the system can be simplified by noticing that MSSM gaugino-mediated interactions of the type  $l + l \rightarrow \tilde{l}\tilde{l}$  are very fast and can be safely assumed to be in thermal equilibrium. This automatically implies that  $\tilde{N}_- = 0$  and  $L = \tilde{L}$ . Thus setting now

$$\begin{aligned} \hat{N}(z) &\equiv N(z) + \tilde{N}_+, \\ \hat{L}(z) &\equiv L(z) + \tilde{L}(z), \end{aligned} \quad (17)$$

the Boltzmann equations driving the system are given by

$$\frac{d\hat{N}}{dz}(z) = -K \sqrt{\frac{1+z_r^2}{z^2+z_r^2}} z^2 (\hat{N} - \hat{N}_{\text{eq}}) [\gamma_d(z) + 2\gamma_s(z) + 4\gamma_t(z)], \quad (18)$$

$$\frac{d\hat{L}}{dz}(z) = K \sqrt{\frac{1+z_r^2}{z^2+z_r^2}} z^2 \left[ \gamma_d(z) \epsilon (\hat{N} - \hat{N}_{\text{eq}}) - \frac{\gamma_d(z) \hat{N}_{\text{eq}} \hat{L}}{4} - \frac{1}{2} \gamma_s(z) \hat{L} \hat{N} - \gamma_t(z) \hat{L} \hat{N}_{\text{eq}} \right], \quad (19)$$

where the  $CP$ -violating parameter  $\epsilon$  is defined as in [8],  $\gamma_d(z) = K_1(z)/K_2(z)$  ( $K_{1,2}$  are Bessel functions of the first kind) and  $\hat{N}_{\text{eq}}(z) = z^2 K_2(z)/2$ . Here, we have included the dominant lepton number violating scattering amplitudes  $\gamma_{s,t}$  proportional to the top Yukawa coupling  $\lambda_t$  and driven by Higgs exchange, which are given by

$$\gamma_{s,t}(z) \equiv \frac{1}{n_{\text{eq}} \Gamma_d} \frac{T}{64\pi^4} \int ds \hat{\sigma}_{s,t}(s) \sqrt{s} K_1 \left( \frac{\sqrt{s}}{T} \right), \quad (20)$$

where  $n_{\text{eq}}(z) = (g/2\pi^2)(M^3/z)K_2(z)$  with  $g = 2$  (either Majorana  $\nu$  or  $\tilde{\nu} + \tilde{\nu}^\dagger$ ) and  $\hat{\sigma}_{s,t}(s) \equiv 3(\alpha_u/4\pi)f_{s,t}(s/M^2)$ ,  $\alpha_u = \lambda_t^2/4\pi$ . In the above equation the functions  $f_{s,t}$  are given by

$$\begin{aligned} f_s(x) &\equiv 3 \left[ f^{(0)}(x) + \frac{f^{(3)}(x)}{2} + f^{(5)}(x) + \frac{f^{(8)}(x)}{2} + \frac{f_{22}(x)}{2} \right], \\ f_t(x) &\equiv \frac{3}{2} \left[ f^{(1)}(x) + f^{(2)}(x) + f^{(4)}(x) + f^{(6)}(x) + f^{(7)}(x) + f^{(9)}(x) + f_{22}(x) \right], \end{aligned} \quad (21)$$

where the functions  $f^{(i)}$  can be read off from equations (C.20–C.30) and (14) of [8]. In our calculation, we include the thermal effect by taking  $a_h \equiv m_H(T)/M$  [9], where  $m_H(T) \simeq 0.4 T$  is the thermal mass for the Higgs/higgsino particles. We remark that

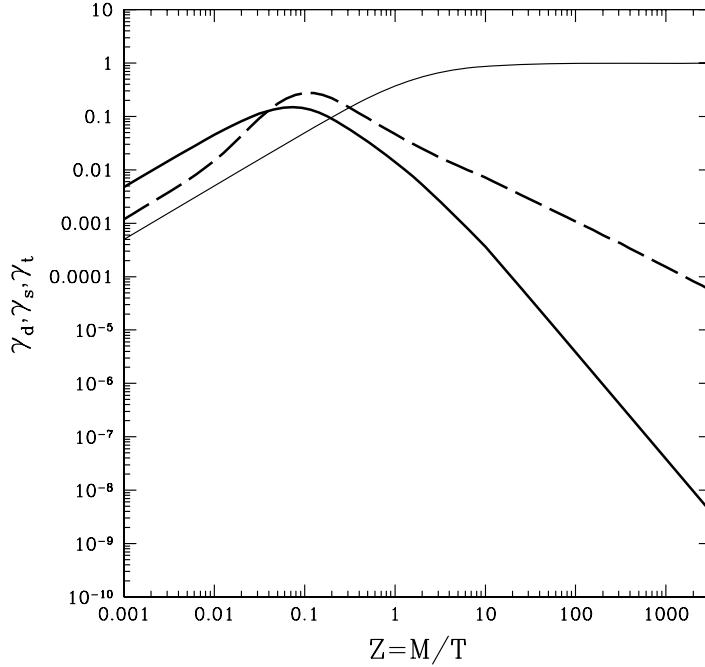


**Figure 1.** Decay and scattering rates  $\gamma_d$  (thin solid line),  $\gamma_s$  (thick solid line),  $\gamma_t$  (thick dashed line) used in the Boltzmann equations (18) and (19), as a function of  $z$ .

in our analysis the difference between bosons and fermions is neglected, as we work in the Boltzmann approximation. The main effect of the quantity  $a_h$  is to regularize the infrared divergence in the t-channel, which shows up in the logarithms in the functions  $f^{(i)}$ . In particular, when  $a_h$  is neglected everywhere with the exception of the logarithms, the functions  $f_{t,s}$  take the simplified form

$$\begin{aligned} f_s &\equiv 6 \frac{x-1}{x}, \\ f_t &\equiv 6 \left[ -1 + \log \frac{x-1+a_h}{a_h} \right]. \end{aligned} \quad (22)$$

However, in our numerical calculations, we kept  $a_h$  everywhere (although equation (22) leads to very similar conclusions). Note that scattering effects may be safely included at the tree level, and at this order of perturbation theory they are  $CP$ -conserving processes.

The effect of thermal corrections on the other masses, as well as on the  $CP$ -violating parameter  $\epsilon$ , has been considered in the literature [9], and can be important, especially at high temperatures. However, in our case the bulk of leptogenesis takes place at temperatures low enough to suppress any sizable effect on the final result, so in the following we will neglect thermal effects, with the exception of the introduction of the coefficient  $a_h(T)$ . The functions  $\gamma_d$  and  $f_{s,t}$  are plotted in figure 1 as a function of  $z$ . Figure 1 shows that the effect of scattering is particularly important at higher temperatures, where the amplitudes  $\gamma_{s,t}$  are larger than  $\gamma_d$ . On the other hand, at lower temperatures the effect of scattering turns out to be negligible.

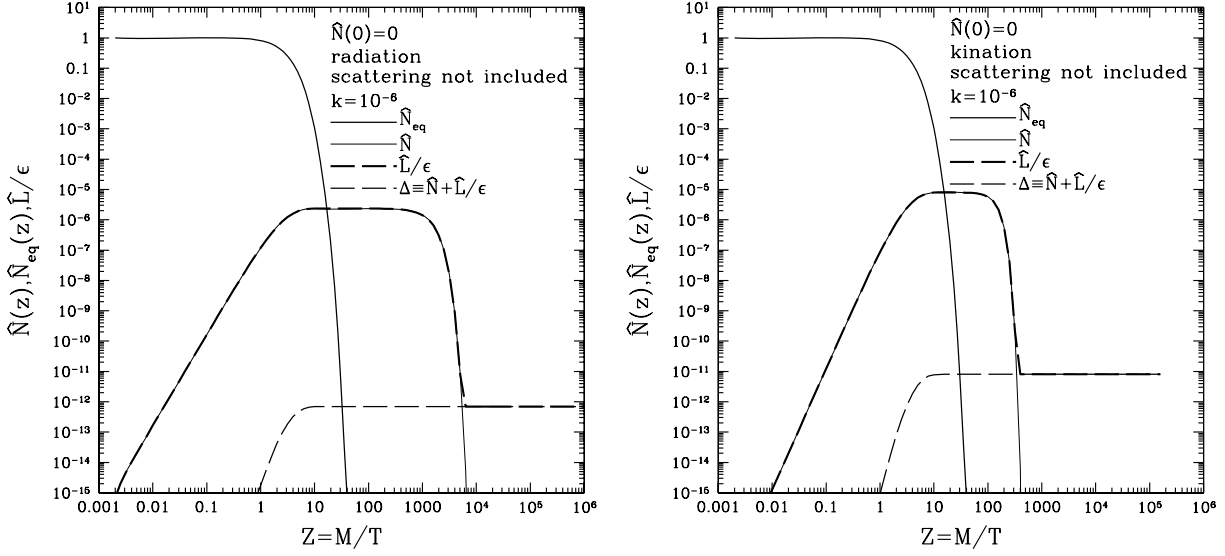


**Figure 2.** Evolution as a function of  $z \equiv M/T$  of the quantities  $\hat{N}$ ,  $\hat{L}/\epsilon$ ,  $\Delta \equiv \hat{N} + \hat{L}/\epsilon$ , for the case  $K = 10^{-6}$ , and neglecting scattering. Left panel: energy density dominated by the radiation field; right panel: energy density dominated by kination.

#### 4. Properties of leptogenesis: kination versus radiation

In this section we discuss the solutions of the Boltzmann equations (18) and (19) for some illustrative examples. We mainly concentrate here on the case of a vanishing initial RHN density,  $\hat{N}(0) = 0$ , and give some comments also for the case  $N(0) = 1$  (initial thermal distribution for the RHN). Besides solving them numerically for the more general cases, it is useful to work out semi-analytic solutions of equations (18) and (19) in the limits  $K \ll 1$  and  $K \gg 1$  in the two cases of radiation domination ( $z_r \ll 1$ ) and kination domination ( $z_r \gg 1$ ).

##### 4.1. Superweak wash-out regime

In the case  $K \ll 1$ , leptogenesis takes place early, when  $z \lesssim 1$  (see the discussion of figures 2 and 3). As a consequence of this, in equation (18) one can neglect  $\hat{N} \ll \hat{N}_{\text{eq}}$ , so that it decouples from equation (19). Setting

$$\Delta \equiv \hat{N} + \frac{\hat{L}}{\epsilon}, \quad (23)$$

one gets for the efficiency  $\eta$  the solution

$$\begin{aligned} \eta \equiv \frac{\hat{L}(\infty)}{\epsilon} &= \Delta(\infty) \simeq K \int_0^\infty z^n \hat{N}_{\text{eq}}(z) (\gamma_d + 2\gamma_s + 4\gamma_t) dz \\ &\simeq K \int_0^\infty z^{n+2} K_2(z) (\gamma_s + 2\gamma_t) = K \hat{I}_n, \end{aligned} \quad (24)$$

with  $\hat{I}_1 \simeq 0.504$ , and  $\hat{I}_2 \simeq 0.921$ , where  $n = 1$  and 2 for radiation and kination domination,



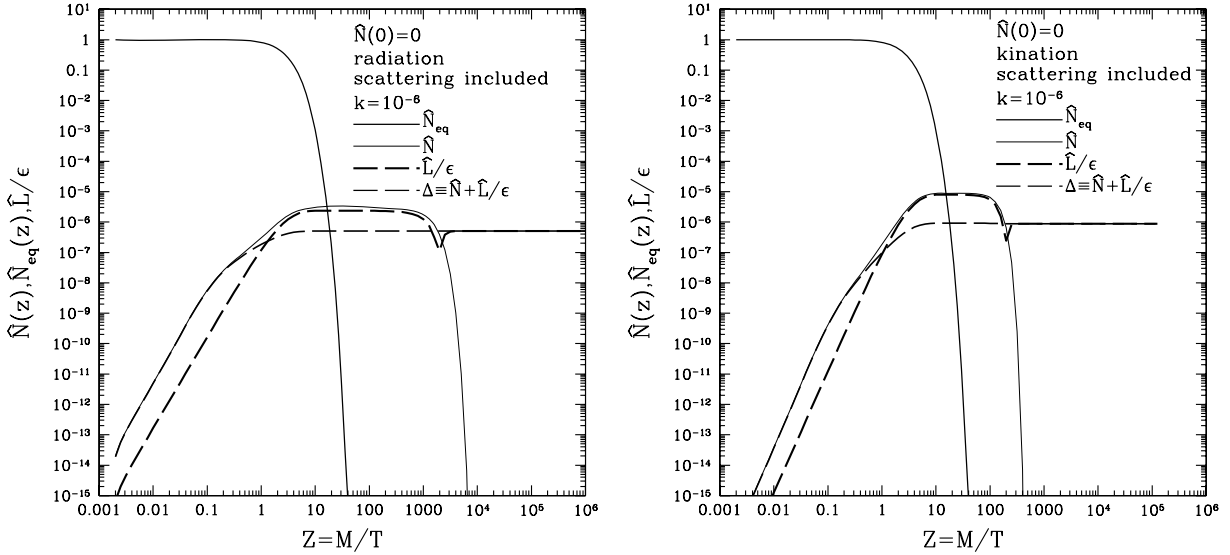


**Figure 3.** The same as in figure 2 with the inclusion of the scattering effect.

respectively. In the second integral of equation (24)  $\gamma_d$  has been dropped, since the integral takes its main contribution at  $z \lesssim 1$  where scattering amplitudes dominate. So, for  $K \ll 1$ , scattering turns out to be essential in determining the efficiency  $\eta$ . Equation (24) is consistent with the result of [11], which in particular showed how  $\eta$  is proportional to  $K^2$  or  $K$ , depending on whether scattering terms are neglected or included, respectively.

To see more in detail the behavior of the numerical solutions of equations (18) and (19) in the two cases of kination and radiation domination, we show them for  $K = 10^{-6}$  in figures 2 and 3. In particular, in the former the scattering effect is neglected, while in the latter it is included. In both figures the evolution of the different quantities  $\hat{N}$ ,  $\hat{L}/\epsilon$  and  $\Delta$  is shown as a function of  $z$ , and the left-hand panel shows the result obtained by assuming  $z_r \ll 1$  ( $n = 1$ ) in the Boltzmann equations (radiation domination), while the right-hand panel is calculated for  $z_r \gg 1$  ( $n = 2$ ) (kination dominated).

Some general features, valid for both kination and radiation, can be realized by comparing these figures. In both cases, at higher temperatures an initial population of RHNs and an early lepton asymmetry are built up. This process is active as long as the initial light states have enough kinetic energy to create RHNs, i.e., as long as  $z = M/T < 1$ . By the time  $z \simeq 1$  and this process stops, RHNs have neither thermalized nor decayed due to their very weak couplings, so both the RHN density and the lepton asymmetry are frozen as can be seen from their evolution in figures 2 and 3 which show a plateau until much later ( $z \gg 1$ ).

In figure 2 where the scattering processes are not included in the calculation, one can see that the asymmetry  $\hat{L}/\epsilon$  tracks closely  $\hat{N}$  until the decay of RHNs. Moreover, when RHNs decay, they produce a lepton asymmetry that cancels the one created earlier due to inverse decays by several orders of magnitude. It is worth noticing here that inverse decay rates are proportional to the densities of initial states, so the inverse decay rate for a particle whose reaction is faster than its anti-particle (due to  $CP$  violation) is suppressed

by the higher depletion in the corresponding population. This implies that the effective amount of  $CP$  violation in the early inverse decay processes is slightly smaller than  $\epsilon$ . On the other hand, when the RHNs decay out of equilibrium at later times the amount of  $CP$  violation is exactly given by  $\epsilon$ . So the lepton asymmetry created later has opposite sign and slightly overshoots the earlier one (actually, the wiggle that is visible in the evolution of  $\hat{L}/\epsilon$  signals a sign change, since it is plotted in absolute value). It is this mismatch that explains why in this plot the asymmetry created at early times by inverse decays is not exactly canceled by RHN decays at later times. Anyway, the final value of the asymmetry is given by a very strong cancellation, and is essentially produced by a second-order back-reaction effect. In particular, it can be seen that, when scattering is neglected,  $\hat{L}/\epsilon \propto K^2$  [11], which implies a strong suppression for  $K \ll 1$ .

The inclusion of scattering processes in the solution of the Boltzmann equations changes the property described above. First of all, due to the higher overall interaction rate, the RHNs are more populated in the first place, and this enhances the final asymmetry. However, the main effect which is active now is due to the presence of s-channel scatterings of the type  $Q + U \rightarrow N + L$ . In fact, this last type of interaction, which is dominant for  $z \lesssim 0.2$  (see figure 1), is (approximately) a  $CP$ -conserving process. This means that it populates  $\hat{N}$  without affecting  $\hat{L}/\epsilon$  (since, for instance,  $\Gamma(Q + U \rightarrow N + L) = \Gamma(\bar{Q} + \bar{U} \rightarrow N + \bar{L})$ ). As a consequence of this, in both panels of figure 3 now the asymmetry  $\hat{L}/\epsilon$  no longer tracks  $\hat{N}$  (this may be appreciated in figure 3 at early times, when  $z \lesssim 0.2$ , and s-channel scattering processes are dominant). When these RHNs decay at later times, they produce a lepton asymmetry that is not canceled by an earlier, specular one, left over by their earlier production. This explains why in figure 3 almost all the asymmetry produced for  $z \lesssim 0.2$  survives until later times, while that created later is washed out. As a consequence of this, including scattering processes the efficiency is much higher and the characteristic drop in the asymmetry when RHNs decay is much less pronounced.

By comparing the two panels of figure 3, one can see the effect of different cosmological models on the evolution of the lepton asymmetry. The final values of the efficiency are quite similar in the two cases. As estimated in equation (24), the difference between kination and radiation in the final asymmetry is expected to be about a factor of 2 for fixed  $K$ . Moreover, the plateau in the evolution of the asymmetry corresponds to a shorter interval in  $z$  in the case of kination compared to radiation: this is due to the fact that, in the time interval given by the RHN lifetime, the Universe is decelerating faster for kination, implying less expansion and cooling, so that the corresponding variation of the  $z$  parameter is smaller.

## 4.2. Strong wash-out regime

For  $K \gg 1$ , the semi-analytic solutions of the Boltzmann equations (18) and (19) can be calculated using the saddle point technique. In this case the bulk of the lepton asymmetry is produced at the decoupling temperature  $z_f$ , determined by the approximate relation

$$z_f^{n+3/2} e^{-z_f} = \frac{2^{7/2}}{K \pi^{1/2}} \quad (25)$$

(where again  $n = 1$  for radiation and  $n = 2$  for kination), which can be approximated by the logarithmic fits

$$\begin{aligned} z_f &\simeq a_n + b_n \ln(K), \\ a_1 &= 1.46; & b_1 &= 1.40, \\ a_2 &= 4.66; & b_2 &= 1.41. \end{aligned} \quad (26)$$

By comparing equations (14) and (26) it is possible to set an upper bound on  $K$ , as anticipated in the previous section. In fact, by fixing  $K$  in both equations and requiring that  $z_f < z_r$  (i.e., that decoupling happens in the regime of kination domination), one gets the inequality

$$z_f \simeq a_2 + b_2 \ln(K) < \sqrt{\left(\frac{63.78}{K} \frac{\tilde{m}}{0.05 \text{ eV}}\right)^2 - 1} = z_r. \quad (27)$$

This numerically implies, for instance,  $K \lesssim 7.6$  for  $\tilde{m} = 0.05 \text{ eV}$ , and  $K \lesssim 5.7$  for  $\tilde{m} = 0.01 \text{ eV}$ . The inequality (27) has no solution for  $K > 1$  when  $\tilde{m} \lesssim 0.004 \text{ eV}$ .

For  $K \gg 1$ , the final value of the efficiency is given by the approximate expression

$$\eta = \frac{\hat{L}(\infty)}{\epsilon} = \hat{N}_{\text{eq}}(z_f) F_{\text{wash-out}}(n, z_f), \quad (28)$$

where

$$\hat{N}_{\text{eq}}(z_f) = \frac{4}{K z_f^n}, \quad (29)$$

and

$$F_{\text{wash-out}}(n, z_f) \simeq \sqrt{\frac{2\pi}{1 - n/z_f}} \exp\left[-\left(1 + \frac{3/2 + n}{z_f}\right)\right]. \quad (30)$$

An example of the numerical solutions of equations (18) and (19) in the strong wash-out regime is shown in figure 4 for  $K = 10$ , in the cases of kination domination (left panel) and radiation domination (right panel). As opposed to the figure 3 case, now RHNs quickly thermalize, and produce a lepton asymmetry when they decouple at  $z \simeq z_f \gg 1$ . In figure 4 the scattering effect is included, but does not affect the final asymmetry, since the latter may develop only at late times when the scattering processes are negligible.

By comparing the two panels one can see that, as implied by equation (26), RHNs stay in thermal equilibrium longer for kination than for radiation. This is explained by the fact that the two models have the same Hubble expansion rate at  $z = 1$  (when  $K$  is defined) but decoupling happens at  $z > 1$ , when the model dominated by kination is decelerating faster and has a slower expansion compared to the case for radiation domination. Moreover, the RHN equilibrium density for  $z > 1$  is further suppressed for kination compared to radiation (see equation (29)). This implies a sizable difference in the final lepton asymmetry between kination and radiation, in contrast to what happens in the case  $K \ll 1$  for which the difference is less pronounced. Note also that, since the RHNs thermalize at  $z \simeq 1$ , erasing any dependence of the final asymmetry on earlier boundary conditions, the calculated efficiency would be the same assuming  $\hat{N}(0) = 1$ .

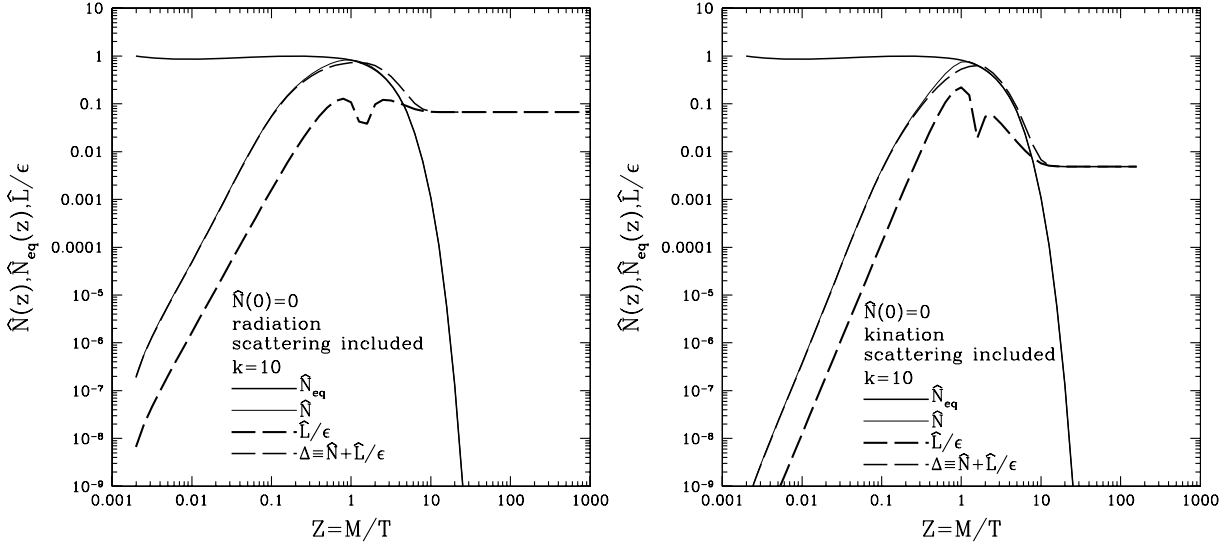


**Figure 4.** The same as in figure 3, but for the case  $K = 10$ .

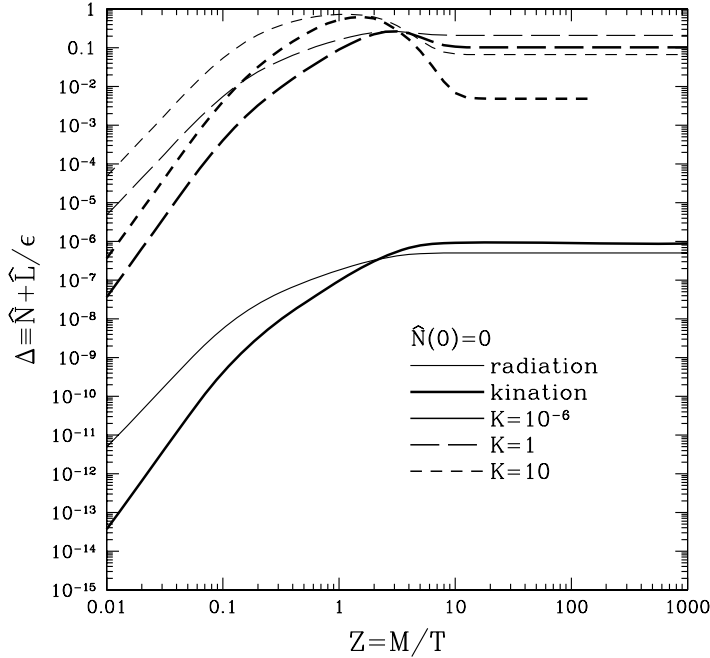


**Figure 5.** Evolution of  $\Delta \simeq \hat{N} + \hat{L}/\epsilon$  as a function of  $z$ , with the boundary condition  $\hat{N}(0) = 0$ . Thin lines = radiation, thick lines = kination. Solid line, long dashes and short dashes for  $K = 10^{-6}$ , 1 and 10, respectively.

In order to summarize the temperature dependence of the solutions of the Boltzmann equations (18) and (19), we present in figure 5 the evolution of  $\Delta$  as a function of  $z$  for  $K = 10^{-6}$  (solid line), 1 (long dashes), 10 (short dashes), for the cases of radiation domination (thin lines) and kination domination (thick lines), and when the boundary condition  $\hat{N}(0) = 0$  is adopted. The same plot for the case  $\hat{N}(0) = 1$  is shown in figure 6.

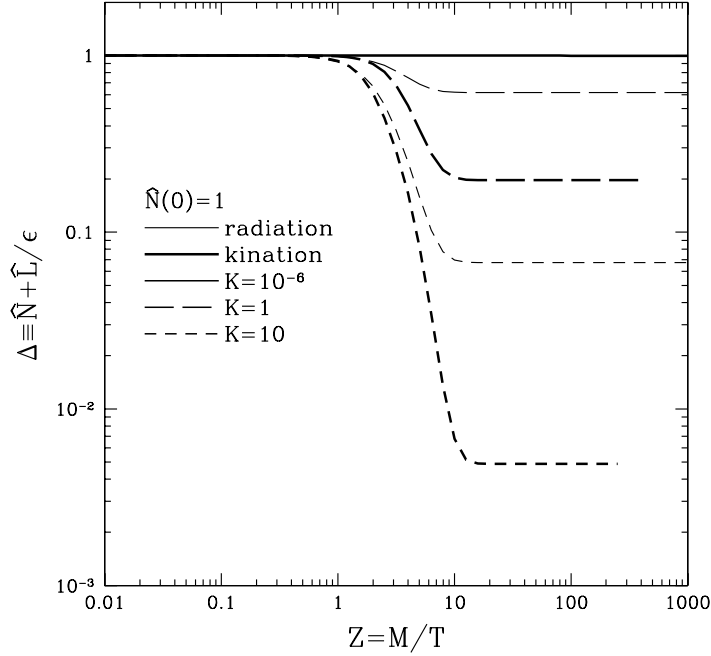


**Figure 6.** The same as in figure 5, but for  $\hat{N}(0) = 1$ .

In the latter case, for  $K \ll 1$  one has  $\Delta = 1$  during the whole range of  $z$ , and both for radiation and kination. This corresponds to the ideal case when the initial equilibrium density of RHNs decays out of equilibrium with efficiency 1. For  $K \gtrsim 1$  and as long as the RHNs reach thermalization, the efficiency is the same as for the case with  $\hat{N}(0) = 0$  already discussed. In particular, as already mentioned, in this case the efficiency for kination is lower compared to that for radiation because of the later decoupling for the RHNs.

### 4.3. The efficiency in terms of $K$ or $(z_r, \tilde{m})$

In figure 7 the efficiency  $\hat{L}/\epsilon$  is plotted as a function of  $K$ . From this figure it is possible to summarize the various properties discussed above, comparing the cases of kination and radiation domination:

- curves for  $\hat{N}(0) = 0$  and  $\hat{N}(0) = 1$  differ at  $K < 1$  (the latter saturating to 1) but coincide for  $K > 1$ ;
- the effect of scattering is important for  $K < 1$ , implying in particular a large increase of the efficiency at very low  $K$ , but a negligible one at  $K > 1$ ;
- for  $K > 1$  the efficiency for kination is about one order of magnitude smaller than for radiation (see equations (25) and (28)); on the other hand the efficiencies are comparable in the two cases for  $K \lesssim 1$  (see equation (23)).

We conclude this section by discussing the phenomenology of leptogenesis as a function of  $T_r$ , defined as the temperature for which the energy density of radiation and that of kination are the same. In figure 8 the efficiency is plotted as a function of the adimensional parameter  $z_r \equiv \sqrt{g_*/g_{*r}} M/T_r$ , for some representative values of the

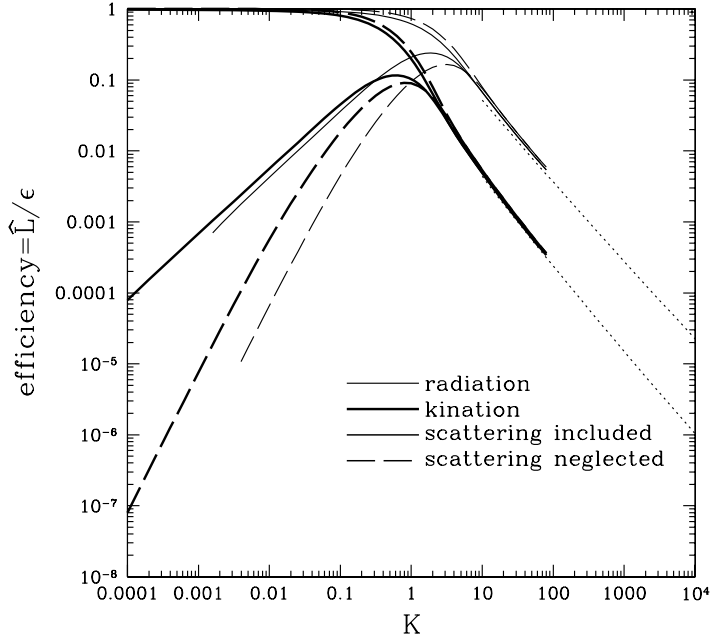


**Figure 7.** The efficiency  $\eta = \hat{L}(z = \infty)/\epsilon$  as a function of  $K$ . Curves that saturate to 1 at  $K \ll 1$  have a thermal initial distribution ( $\hat{N}(0) = 1$ ) for RHNs, while those that vanish when  $K \ll 1$  have  $\hat{N}(0) = 0$ . Thick lines: kination; thin lines: radiation; solid lines: scattering included; long dashes: scattering neglected. Dots: approximations given for  $K \gg 1$  by equations (26), (28), (29) and (30).

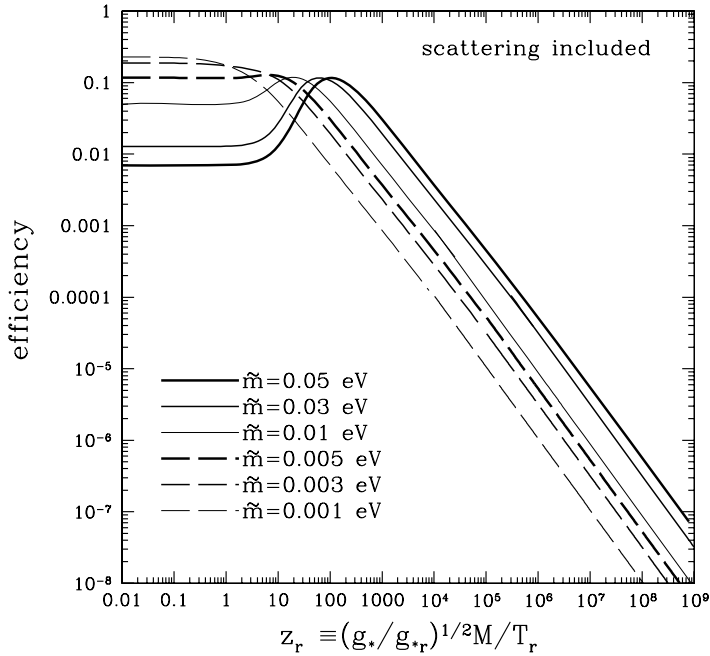


**Figure 8.** The efficiency as a function of  $z_r \equiv \sqrt{g_*/g_{*r}} M/T_r$ , for  $N(0) = 0$  and for several values of  $\tilde{m}$ . A smooth transition between radiation domination (the plateau at  $z_r \lesssim 1$ ) and kination domination ( $z_r \gtrsim 100$ ) is clearly visible.

neutrino mass scale  $\tilde{m}$ . In this figure it is possible to see a smooth transition from radiation domination ( $z_r \ll 1$ ) to kination domination ( $z_r \gg 1$ ), and the following characteristic behaviors:

- Superweak wash-out regime with  $z_r \gg 100$ . Assuming  $T_r \gtrsim 1$  MeV and taking into account the corresponding constraint  $M \lesssim 10^5$  (see equation (10)) one gets the upper bound  $z_r \lesssim 4.5 \times 10^8$ . Assuming for instance  $\tilde{m} = 0.05$  eV, this value of  $z_r$  corresponds in figure 8 to  $K \lesssim \hat{L}/\epsilon \simeq 10^{-7}$ . This situation has to be compared to the standard picture in which the energy density is dominated by radiation, corresponding, for the same curve, to the plateau at  $z_r \ll 1$ , for which  $K \simeq 64$  and  $\hat{L}/\epsilon \simeq 0.007$ . So, if kination dominates the energy density of the Universe until nucleosynthesis, the corresponding efficiency for leptogenesis is suppressed by almost six orders of magnitude compared to the standard cosmology with radiation domination.
- Increased efficiency with  $1 \lesssim z_r \lesssim 100$ . However, from the same figure it is possible to see that very different scenarios are possible by assuming  $T_r \gg 1$  MeV. For instance, when  $\tilde{m} \gtrsim 0.01$  eV the efficiency in the case of kination can be even larger compared to that for radiation for  $1 \lesssim z_r \lesssim 100$ . This can be explained by the fact that, for this range of  $\tilde{m}$ , the radiation dominated situation corresponds to a regime of strong washout,  $K > 10$ , while for kination it is possible to have  $K \simeq 0.1-1$ , i.e. right in the interval that corresponds to a maximal efficiency. For instance, in figure 8 the maximum at  $z_r \simeq 100$  for the curve with  $\tilde{m} = 0.05$  eV corresponds to  $K \simeq 0.63$ , which in figure 7 is the value of  $K$  where the efficiency is maximal for kination domination. On the other hand, this mechanism gets much more efficient and  $\hat{L}/\epsilon$  is strongly suppressed for  $z_r \gg 10^3$ . Note that the possibility of increasing the efficiency in the case of kination domination compared to radiation is easier for somewhat larger values of  $\tilde{m}$ . In fact, if one takes  $\tilde{m} < 0.05$  eV, the value of  $K$  in the radiation dominated case becomes smaller. According to figure 7, when  $K \simeq 1$  the efficiency for radiation is maximal, and this corresponds to  $\tilde{m} \simeq 8 \times 10^{-4}$  eV. So, for  $\tilde{m} < 8 \times 10^{-4}$  eV, adding a period of kination always implies a lower efficiency. We point out that, for  $\tilde{m} = 0.05$  eV, the maximal efficiency achieved in figure 8 at  $z_r \simeq 100$  is about a factor 30 larger than the value corresponding to radiation domination ( $z_r = 0$ ). In particular, assuming a hierarchical spectrum for the heavy neutrino masses, this would imply a lower bound to  $M$  a factor of 30 smaller as compared to the standard case [9, 11].

## 5. Conclusions

We have discussed leptogenesis in the context of a cosmological model where the energy density of the early Universe is dominated by the kinetic term of a quintessence field during some epoch of its evolution. This assumption may lead to very different conclusions compared to the case of the standard cosmology, where the energy density of the Universe is dominated by radiation.

We have adopted as a free parameter the temperature  $T_r$  above which kination dominates over radiation, and shown that when  $T_r$  is set to its minimal value required by nucleosynthesis,  $T_r \simeq 1$  MeV, gauge interactions can thermalize only at a temperature  $T \lesssim 10^5$  GeV, so that the RHN mass  $M \simeq T$  needs to be relatively light. This constraint

is relaxed for higher values of  $T_r$ . Moreover, irrespective of  $T_r$ , we always find a sufficient window above the electroweak temperature  $T \sim 100$  GeV for the sphaleron transition to thermalize and thus allow conversion of the lepton asymmetry to the observed baryon asymmetry.

When the RHN Yukawa coupling is fixed to get the observed neutrino mass scale  $\simeq 0.05$  eV, in standard cosmology leptogenesis proceeds in the strong wash-out regime,  $K \gg 1$ . In contrast, in kination leptogenesis all situations between the strong and the superweak wash-out regimes are equally viable, by varying  $T_r$ . However, the effect of kination turns out to be either negligible or absent for models for which  $K \gtrsim 10$  since the RHNs decay when radiation domination has already settled.

The weak wash-out regime is attained when  $z_r \simeq M/T_r \gg 100$  for which the final efficiency for leptogenesis is approximately given by  $\eta \simeq K \simeq (64/z_r)(\tilde{m}/0.05 \text{ eV})$ , and can be several orders of magnitude smaller than that in the case of radiation domination for fixed  $\tilde{m}$ . In this latter case the efficiency for leptogenesis is strongly suppressed, but can still explain the baryon asymmetry observed in the Universe assuming a resonant  $CP$  asymmetry of order 1. In this case we have stressed the importance of s-channel scatterings driven by the top Yukawa coupling, which are the dominant process for creating RHNs at high temperatures, and so enhance the leptogenesis efficiency by orders of magnitude in models where a vanishing initial RHN density is assumed. We remark that, in the case of kination domination, the condition  $\eta \gtrsim 2.5 \times 10^{-8}$  for a successful leptogenesis, obtained by assuming a resonant  $CP$  asymmetry  $\epsilon = 1$  in the relation  $Y_{\tilde{L}} = 4 \times 10^{-3} \epsilon \eta \approx 10^{-10}$ , requires the upper bound on the RHN mass  $M \lesssim 2.4 \times 10^6 \text{ GeV} (T_r/\text{MeV})(\tilde{m}/0.05 \text{ eV})$ , which is compatible to the condition of equation (10) for  $T_r \sim 1$  MeV. On the other hand, when  $1 \lesssim z_r \lesssim 100$  kination stops dominating at a time which is not much later than when leptogenesis takes place: in this case, if  $\tilde{m} \gtrsim 0.01$  eV, leptogenesis proceeds with  $0.1 \lesssim K \lesssim 1$ , in a regime where the efficiency is even better than that for the case of radiation domination. We point out that in this case thermal leptogenesis can proceed for a hierarchical spectrum of heavy neutrino masses, and for this scenario the lower bound on the RHN mass  $M$  can be relaxed up to a factor of 30 compared to the standard case [9, 11].

We conclude that kination and leptogenesis can indeed be compatible with each other, and that this scenario opens up a wide range of possibilities. Typically, kination domination turns out to be less favorable for thermal leptogenesis than in the standard scenario, since it implies very small efficiencies that require a resonant enhancement of the  $CP$  asymmetry [12] in order to explain the observed baryon asymmetry. However, for a limited range of the parameters, this situation is reversed. The relative phenomenology can be parametrized as a function of only two parameters,  $z_r \equiv \sqrt{g_*/g_{*r}} M/T_r$  and  $\tilde{m}$ .

## Acknowledgment

We thank D Chung for useful discussions.

## References

- [1] Caldwell R R, Dave R and Steinhardt P J, 1998 *Phys. Rev. Lett.* **80** 1582 [SPIRES] [astro-ph/9708069]
- [2] Steinhardt P J, Wang L M and Zlatev I, 1999 *Phys. Rev. D* **59** 123504 [SPIRES] [astro-ph/9812313]
- [3] Kamionkowski M and Turner M S, 1990 *Phys. Rev. D* **42** 3310 [SPIRES]
- Salati P, 2003 *Phys. Lett. B* **571** 121 [SPIRES] [astro-ph/0207396]
- Rosati F, 2003 *Phys. Lett. B* **570** 5 [SPIRES] [hep-ph/0302159]



- Profumo S and Ullio P, 2003 *J. Cosmol. Astropart. Phys.* **JCAP11(2003)006** [SPIRES] [[hep-ph/0309220](#)]  
 Pallis C, 2005 *J. Cosmol. Astropart. Phys.* **JCAP10(2005)015** [SPIRES] [[hep-ph/0503080](#)]  
 Barenboim G and Lykken J D, 2006 *J. High Energy Phys.* **JHEP12(2006)005** [SPIRES] [[hep-ph/0608265](#)]  
 Chung D J H, Everett L L, Kong K and Matchev K T, 2007 *Preprint* [hep-ph/0706.2375](#)  
 [4] Chung D J H, Everett L L and Matchev K T, 2007 *Preprint* [hep-ph/0704.3285](#)  
 [5] Fukugita M and Yanagida T, 1986 *Phys. Lett. B* **174** 45 [SPIRES]  
 Covi L, Roulet E and Vissani F, 1996 *Phys. Lett. B* **384** 169 [SPIRES] [[hep-ph/9605319](#)]  
 [6] Davidson S and Ibarra A, 2002 *Phys. Lett. B* **535** 25 [[hep-ph/0202239](#)]  
 [7] Arnold P, Son D and Yaffe L G, 1997 *Phys. Rev. D* **55** 6264 [SPIRES] [[hep-ph/9609481](#)]  
 Bodeker D, 1998 *Phys. Lett. B* **426** 351 [SPIRES] [[hep-ph/9801430](#)]  
 Moore G D, Hu C and Muller B, 1998 *Phys. Rev. D* **58** 045001 [SPIRES] [[hep-ph/9710436](#)]  
 [8] Plümacher M, 1998 *Nucl. Phys. B* **530** 207 [SPIRES] [[hep-ph/9704231](#)]  
 [9] Giudice G F, Notari A, Raidal M, Riotto A and Strumia A, 2004 *Nucl. Phys. B* **685** 89 [SPIRES] [[hep-ph/0310123](#)]  
 [10] Buchmuller W and Plumacher M, 2001 *Phys. Lett. B* **511** 74 [SPIRES] [[hep-ph/0104189](#)]  
 [11] Buchmuller W, Di Bari P and Plümacher M, 2005 *Ann. Phys., NY* **315** 305 [SPIRES] [[hep-ph/0401240](#)]  
 [12] Pilaftsis A, 1997 *Phys. Rev. D* **56** 5431 [SPIRES] [[hep-ph/9707235](#)]  
 Pilaftsis A and Underwood T E J, 2004 *Nucl. Phys. B* **692** 303 [SPIRES] [[hep-ph/0309342](#)]  
 Turzyski K, 2004 *Phys. Lett. B* **589** 135 [SPIRES] [[hep-ph/0401219](#)]  
 González F R, Joaquim F R and Nobre B M, 2004 *Phys. Rev. D* **70** 085009 [SPIRES] [[hep-ph/0311029](#)]  
 Ahn Y H, Kang S K, Kim C S and Lee J, 2007 *Phys. Rev. D* **75** 013012 [SPIRES] [[hep-ph/0610007](#)]  
 Chun E J and Turzyski K, 2007 *Preprint* [hep-ph/0703070](#)